

Effects of Cr underlayer and Pt buffer layer on the interfacial structure and magnetic characteristics of sputtered FePt films

An-Cheng Sun^{a,b}, Jen-Hwa Hsu^{a,b,*}, H.L. Huang^{a,b}, P.C. Kuo^{a,c}

^aCenter for Nanostorage Research, National Taiwan University, Taipei 106, Taiwan

^bDepartment of Physics, National Taiwan University, Taipei 106, Taiwan

^cDepartment of Materials Science and Engineering, National Taiwan University, Taipei 106, Taiwan

Available online 3 March 2006

Abstract

This work develops a new method for growing L1₀ FePt(001) thin film on a Pt/Cr bilayer using an amorphous glass substrate. Semi-coherent epitaxial growth was initiated from the Cr(002) underlayer, continued through the Pt(001) buffer layer, and extended into the L1₀ FePt(001) magnetic layer. The squareness of the L1₀ FePt film in the presence of both a Cr underlayer and a Pt buffer layer was close to unity as the magnetic field was applied perpendicular to the film plane. The single L1₀ FePt(111) orientation was observed in the absence of a Cr underlayer. When a Cr underlayer is inserted, the preferred orientation switched from L1₀ FePt(111) to L1₀ FePt(001) and the magnetic film exhibited perpendicular magnetic anisotropy. However, in the absence of an Pt intermediate layer, the Cr atoms diffused directly into the FePt magnetic layer and prevented the formation of the L1₀ FePt(001) preferred orientation. When a Pt buffer layer was introduced between the FePt and Cr underlayer, the L1₀ FePt(001) peak appeared. The thickness of the Pt buffer layer also substantially affected the magnetic properties and atomic arrangement at the FePt/Pt and Pt/Cr interfaces.

© 2006 Elsevier B.V. All rights reserved.

PACS: 81.15.C; 75.60.G; 75.70.K

Keywords: Magnetic perpendicular recording; FePt films; Pt buffer layer; Cr underlayer

1. Introduction

CoCr-base alloy thin films are widely employed in longitudinal magnetic recording media. The $M_r t$ product of the media must be small to increase the linear density of magnetic recording, reduce the media noise, and improve the signal to noise ratio (SNR) [1]. ($M_r t$ is the product of remanent magnetization M_r and media thickness t .) The reduction in thickness of the media is always accompanied by shrinkage of the grain, causing thermally unstable magnetization at high linear density with a very large demagnetizing field H_d . Antiferromagnetically coupled (AFC) magnetic recording media have been developed to improve the thermal stability of longitudinal media [2]. The

$M_r t$ of AFC media can be reduced without a decrease in the grain volume [1–3]. Therefore, a high-density recording of 200 G/in² could be attained in AFC media. In future ultra-high-density magnetic recording applications, the AFC recording method will not be used because it yields a high H_d in the longitudinal direction and a minimal stable grain size that increases as the thickness of the media decreases. The perpendicular magnetic recording (PMR) method has been proposed to solve these problems of longitudinal media [4]. In PMR, the direction of magnetization is perpendicular to the film plane. If the surface area of the recording bit is reduced, the volume of the recording bit can still be maintained by increasing the medium thickness. Accordingly, the demagnetized field can be reduced to stabilize the magnetic moments [5].

FePt thin film with a tetragonal L1₀ structure and a (001) texture perpendicular to the film plane is a good candidate for perpendicular magnetic recording medium. The uniaxial magnetocrystalline anisotropic energy of the

*Corresponding author. Department of Physics, National Taiwan University, Taipei 106, Taiwan. Tel.: +886 2 33665162; fax: +886 2 33665892.

E-mail address: jhhsu@phys.ntu.edu.tw (J.-H. Hsu).

$L1_0$ FePt phase is close to 10^8 erg/cm³, which is 50 times greater than that of CoCr-based alloy thin films [6]. Unfortunately, the preferred orientation of the deposited $L1_0$ FePt film is usually (1 1 1), so the easy axis is tilted 35° from the film plane. In a perpendicular recording medium, the preferred orientation of the $L1_0$ FePt film must be with the (0 0 1) plane parallel to the film plane, making the easy crystallization axis [0 0 1] perpendicular to the film plane.

Some methods for preparing an ordered $L1_0$ FePt (0 0 1) texture have been developed [7]. In these fabrication processes, MgO was extensively utilized to promote the preferred orientation with FePt(0 0 1) parallel to the film plane, because the lattice mismatch of the FePt(0 0 1)[1 0 0]/MgO(0 0 2)[1 0 0] planes is around 9.07% [7]. Therefore, the MgO (0 0 2) substrate or MgO (0 0 2) thin film can induce the $L1_0$ FePt (0 0 1) texture. However, the cost of using an MgO(0 0 2) substrate is extremely high and the fabrication temperature of the MgO(0 0 2) thin film always exceeds 500 °C [8], limiting the adoption of MgO in the magnetic recording industry.

In this investigation, a Pt buffer layer and a Cr underlayer were used to induce the preferred orientation with $L1_0$ FePt (0 0 1) parallel to the film plane. This work examines the mechanism of formation and the interfacial characteristics of an ordered $L1_0$ FePt(0 0 1) film on a Pt/Cr bilayer.

2. Experimental

All films were fabricated on preheated 7059 corning glass substrates by conventional DC magnetron sputtering in an ultra-high vacuum-sputtering chamber. The substrate was heated to 350 °C to prepare the Cr underlayer and the Pt buffer layer. The deposition temperature of the FePt magnetic layer was set to 450 °C to overcome the

order–disorder transformation energy barrier to yield the $L1_0$ FePt phase [9]. The thickness of the films was measured by atomic force microscopy (AFM). The crystal structure and the cross-sectional microstructures of the films were investigated by X-ray diffraction (XRD) using Cu-K α radiation and 300 keV high-resolution transmission electron microscopy (HRTEM). The chemical composition of the magnetic FePt alloy layer was determined by energy-dispersive X-ray diffractometry (EDS), which revealed that the composition was Fe₄₈Pt₅₂. The element depth profiles of the films were investigated by Auger electron spectroscopy (AES). Magnetic properties were measured by a vibrating sample magnetometer (VSM) at room temperature.

3. Results and discussion

In our previous study [10], the magnetic FePt film with an ordered $L1_0$ FePt(0 0 1) preferred orientation was prepared on a Pt/Cr bilayer using glass substrate. The thicknesses of the Cr underlayer and the Pt intermediate layer were 90 and 2 nm, respectively. Fig. 1(a) displays an XRD pattern, which includes peaks from the Cr(0 0 2) reflection plane and (0 0 1) and (0 0 2) superlattice planes of the $L1_0$ FePt(0 0 1) phase. The FePt(0 0 1) texture was preserved throughout the $L1_0$ FePt layer by epitaxial growth from the Cr(0 0 2) underlayer. Additionally, the magnetic FePt film has been found to exhibit perpendicular magnetic anisotropy with an out-of-plane squareness (M_r/M_s) of about 1, as shown in Fig. 1(b). The saturation magnetization (M_s) could reach 700 emu/cm³. The easy axis of the film was perpendicular to the film plane.

The thickness of the Cr underlayer d was varied from 0 to 110 nm, while the film thickness of the FePt layer and Pt layer was fixed at 20 and 2 nm, respectively, to explore the

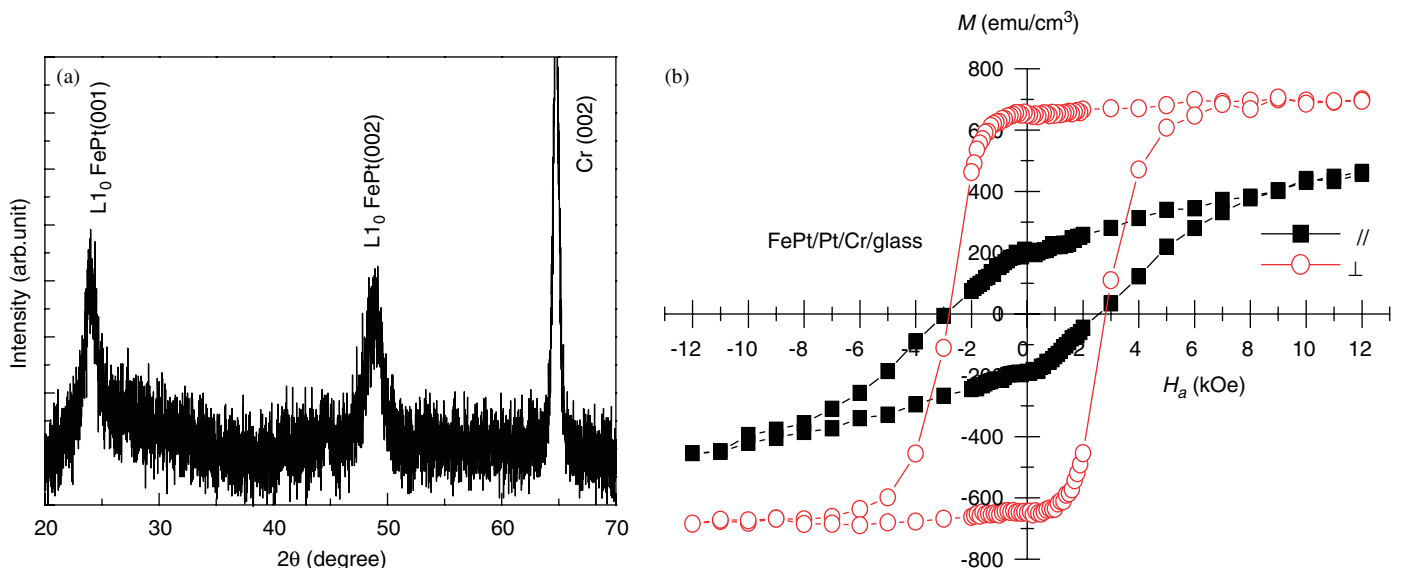


Fig. 1. (a) X-ray diffraction pattern and (b) M – H loop of FePt(20 nm)/Pt(2 nm)/Cr(90 nm) trilayer film.

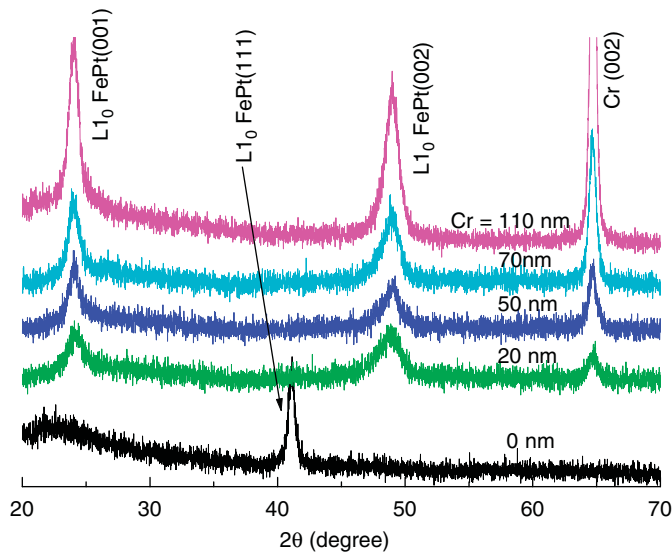


Fig. 2. The X-ray diffraction patterns of FePt/Pt/Cr trilayer films with various Cr underlayer thickness.

effect of the Cr underlayer. Fig. 2 depicts the XRD patterns of the FePt/Pt/Cr trilayers with Cr underlayers of various thicknesses. It shows that only a single $L1_0$ FePt(111) orientation was obtained when no Cr underlayer was present, because the lattice constant of the FCC Pt(111) plane is close to that of the FCT FePt(111) plane. The FePt layer will be epitaxially grown along the Pt(111) plane, yielding an FePt(111)-textured film. When the Cr underlayer was incorporated, $L1_0$ FePt(001) and Cr(002) peaks were found instead. The FePt(111) peak disappeared and the intensity of the FePt(001) and Cr(002) peaks increased with the thickness of the Cr underlayer, indicating that the preferred orientation of the $L1_0$ FePt grains switched from FePt(111) to FePt(001) as the Cr underlayer was added. The FePt(001) texture was originated from the Cr(002) plane.

Fig. 3 plots the squareness (M_r/M_s) and the out-of-plane coercivity ($H_{c\perp}$) of the FePt/Pt/Cr trilayer as a function of the Cr underlayer. In the absence of a Cr underlayer, the in-plane squareness (S_{\parallel}) was about 0.67 higher than the out-of-plane squareness ($S_{\perp} \sim 0.59$). When $d = 20$ nm, S_{\perp} increased dramatically to 0.92, and S_{\parallel} dropped to 0.42, suggesting that the perpendicular magnetic anisotropy dominated at $d = 20$ nm. S_{\perp} always exceeded 0.85, even when the thickness of the Cr underlayer was increased to 110 nm. S_{\parallel} fell as the thickness of the Cr underlayer increased; S_{\parallel} was largest (0.67) at 0 nm and it declined to about 0.16 at $d = 110$ nm. The increase in the thickness of the Cr underlayer reinforced the perpendicular FePt(001) orientation. The out-of-plane coercivity ($H_{c\perp}$) was also found to depend on the thickness of the Cr underlayer. $H_{c\perp}$ was largest for the FePt/Pt bilayer structure, with $d = 0$. However, FePt/Pt bilayer did not exhibit perpendicular FePt(001) anisotropy. Only the FePt/Pt/Cr trilayer system exhibited an FePt(001) texture with large $H_{c\perp}$. $H_{c\perp}$ increased from 2.8 to 3.6 kOe as the thickness of the Cr

underlayer increased from 20 to 70 nm. $H_{c\perp}$ decreases considerably as $d > 70$ nm. These results were consistent with the results of a microstructure study [11]. The TEM plane view images of FePt/Pt/Cr trilayer films showed some black and white stripes in FePt/Pt/Cr films with a 90 nm Cr underlayer, but not in such films with a 70 nm Cr underlayer. The stripes might be caused by phase separation or local compositional inhomogeneity, which may reduce the magnetic anisotropy and out-of-plane coercivity.

The effects of the thickness of the Pt buffer layer on the microstructure and magnetic characteristics of the FePt/Pt/Cr trilayer were also studied. Fig. 4 displays XRD patterns of the FePt/Pt/Cr trilayer with various Pt buffer layer thicknesses. The thicknesses of the FePt layer and the Cr underlayer were 20 and 90 nm, respectively. Without a Pt buffer layer, the ordered FePt(001) phase was difficult to

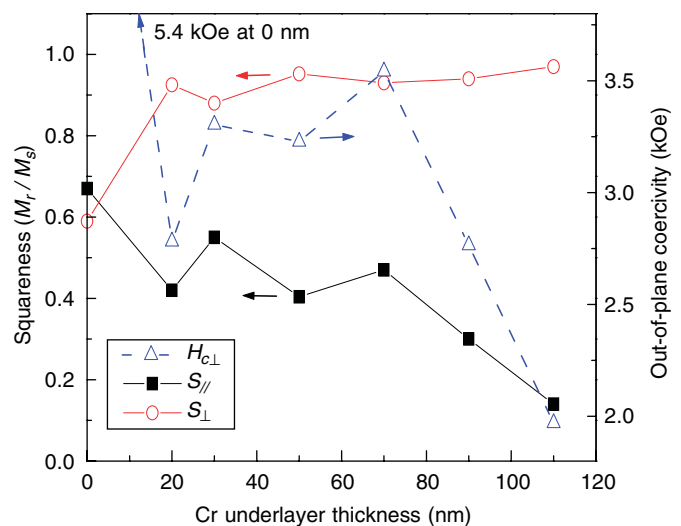


Fig. 3. The squareness (M_r/M_s) and out-of-plane coercivity ($H_{c\perp}$) of FePt/Pt/Cr trilayer as a function of the Cr underlayer thickness.

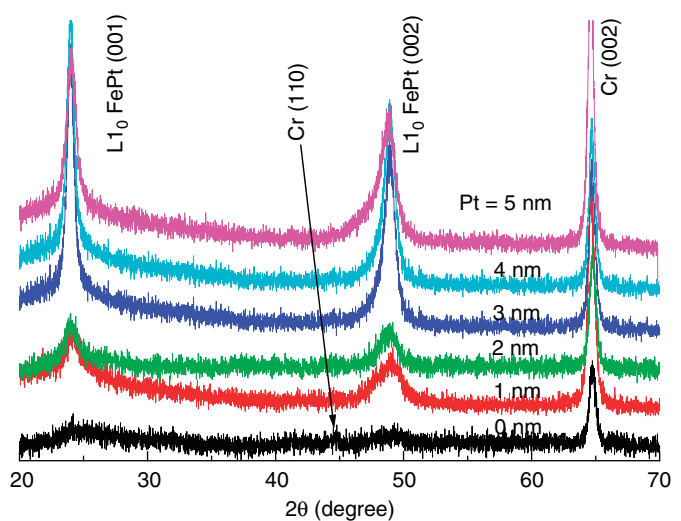


Fig. 4. The X-ray diffraction patterns of FePt/Pt/Cr trilayer with various Pt buffer layer thicknesses.

identify. The intensity of the Cr(002) peak was low and the Cr(110) peak was present. This result was unexpected. The lattice misfit of the Cr(002)/FePt(001) planes is only 5.8%; so the ordered FePt(001) texture is expected to grow epitaxially with the crystal orientation Cr(002)[110]/FePt(001)[100]. However, this did not occur. The TEM cross-section image revealed that the epitaxial growth of FePt(001) on the Cr(002)/FePt(001) interface was disrupted [10].

When the Pt layer was inserted between the magnetic FePt layer and the Cr underlayers, the FePt(001) texture appeared, and the intensity of the Cr(002) peak was markedly increased. This result revealed that good epitaxial growth started from the Cr underlayer and extended to the Pt layer and the FePt magnetic layer. The lattice constant of Pt is 3.92 Å, which is between the 4.08 Å of Cr(002) and the 3.85 Å of FePt(100). Hence, the intermediate Pt layer substantially reduces the strains at the FePt/Pt and Pt/Cr interfaces. Accordingly, the epitaxial growth can continue over a long distance. Consequently, the preferred orientation of the L1₀ FePt phase was (001) and the film exhibited perpendicular magnetic anisotropy. In Fig. 4, the intensity of the FePt(001) peak was highest when the thickness of the Pt layer was 3 nm. Further increasing the thickness of the Pt layer reduced the height of the FePt(001) peak. The FePt(002) peak became boarder as the Pt layer thickness increased above 3 nm, perhaps because of the reduction of the order–disorder transformation of FePt, and the associated decrease in the amount of L1₀ FePt phase as the thickness of the Pt layer was increased. Interfaces of the FePt/Pt/Cr trilayer thin films with 2 and 4 nm Pt buffer layers were examined to understand the drop of the ordering rate of FePt. Fig. 5 displays the TEM cross-sectional images with Pt layers of thicknesses 2 and 4 nm. The black and white arrows indicate the mismatch dislocation at the Pt/Cr and FePt/Pt interfaces, respectively. The mismatch dislocation can modulate the mismatch strain energy and cause the films to grow epitaxially and well at the interface [8]. When the thickness of the Pt layer was 2 nm, many dislocations were present at the FePt/Pt/Cr interfaces, as shown in Fig. 5(a). However, when the thickness of the Pt buffer layer was increased to 4 nm, mismatch dislocations at the interface were difficult

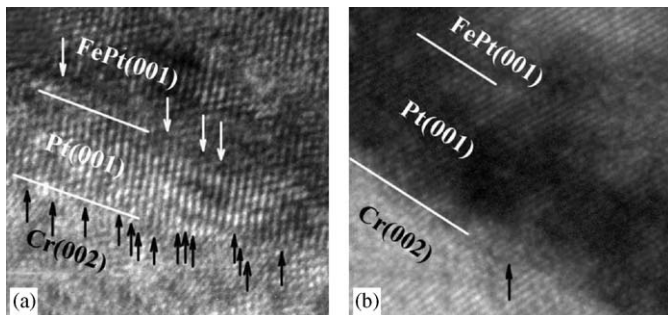


Fig. 5. TEM cross-sectional images with (a) 2 nm and (b) 4 nm Pt layer of FePt/Pt/Cr trilayer.

to identify, as shown in Fig. 5(b). This result indicates that the lattice misfit strain energy is released gradually to yield a thicker Pt layer. The introduction of defects in the FePt thin film may promote the order–disorder transformation and reduce the ordering temperature [11,12]. The ordering temperature of a thicker Pt buffer layer (4 nm) was high because few mismatch dislocations were present. Therefore, a thicker Pt layer is associated with a less intense L1₀ FePt(001) peak in the XRD pattern (see Fig. 4).

Fig. 6 plots the squareness and out-of-plane $H_{c\perp}$ versus the thickness of the Pt layer. S_{\parallel} exceeded S_{\perp} when the Pt layer was thinner than 2 nm, suggesting that the in-plane magnetic anisotropy was greater than the perpendicular anisotropy. S_{\perp} was always higher than 0.9 and S_{\parallel} was smaller than 0.3 as the thickness of the Pt layer increased. Perpendicular magnetic anisotropy was realized if the Pt layer was thicker than 2 nm. Without a Pt buffer layer, $H_{c\perp}$ was only approximately 1.8 kOe. The AES element depth profile analysis revealed that the Cr atoms diffused directly into the FePt layer and distorted the FePt(001) texture [10]. The saturation magnetization (M_s) of the FePt/Cr bilayer was also reduced to be about 450 emu/cm³. A thin Pt buffer layer (2 nm) was found to suffice to impede the diffusion of the Cr atoms from the Cr underlayer into the FePt magnetic layer, yielding a better FePt(001) orientation. The effect of the Pt buffer layer on the magnetic characteristics can be described as follows. $H_{c\perp}$ increased from 1.8 to 3.0 kOe as the Pt layer thickness increased from 0 to 3 nm, and then declined to 2.5 kOe as the thickness of the Pt layer was further increased from 3 to 5 nm. The fall in $H_{c\perp}$ as the Pt layer thickness increased above 3 nm, and was related to the reduction in interfacial dislocations (Fig. 5(b)).

4. Conclusion

The epitaxial growth of L1₀ FePt thin films on the Pt/Cr bilayer with an amorphous glass substrate was studied.

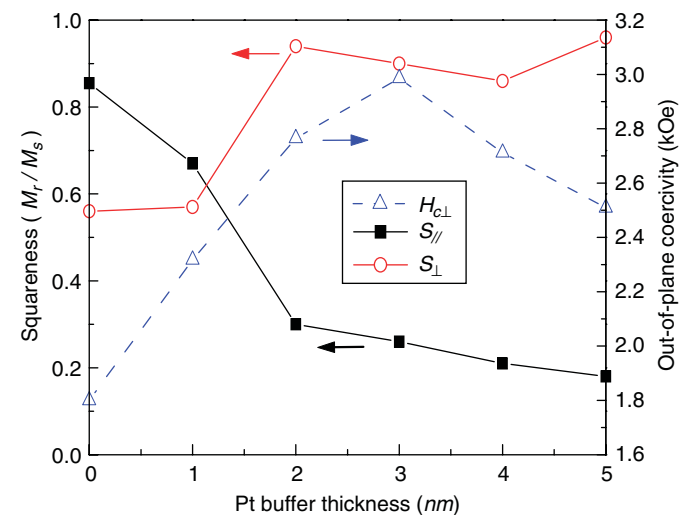


Fig. 6. The squareness (M_r/M_s) and out-of-plane coercivity ($H_{c\perp}$) of FePt/Pt/Cr trilayer films as a function of the thickness of Pt buffer layer.

Perpendicular magnetic anisotropy was present only with both a Cr underlayer and a Pt buffer. Epitaxial growth was initiated from the Cr(002) underlayer, continued through the Pt buffer layer, and extended into the $L1_0$ FePt(001) magnetic layer. Without a Pt buffer layer, the Cr atoms diffused directly into the FePt magnetic layer, eliminating the perpendicular magnetic anisotropy and preventing the epitaxial growth of the FePt magnetic layer. However, a thicker Pt buffer layer is responsible for the modulation of the mismatch strain energy, reducing the degree of interfacial dislocation at FePt/Pt/Cr interfaces. Hence, the order–disorder transformation energy of FePt cannot be lowered efficiently, resulting in the reduction of the perpendicular coercivity.

Acknowledgements

This work was supported by the Ministry of Economic Affairs of Taiwan, ROC, through Grant No. 93-EC-17-A-08-S1-0006.

References

- [1] E.N. Abarra, A. Inomata, H. Sato, I. Okamoto, Y. Mizoshita, Appl. Phys. Lett. 77 (2000) 2581.
- [2] Eric E. Fullerton, D.T. Margulies, M.E. Schabes, M. Carey, B. Gurney, A. Moser, M. Best, G. Zeltzer, K. Rubin, H. Rosen, M. Doerner, Appl. Phys. Lett. 77 (2000) 3806.
- [3] M.E. Schabes, E.E. Fullerton, D.T. Margulies, IEEE Trans. Magn. 37 (2001) 1432.
- [4] S. Iwasaki, Y. Nakamura, K. Ouchi, IEEE Trans. Magn. 15 (1979) 1456.
- [5] Toshiyuki Suzuki, IEEE Trans. Magn. 20 (1984) 675.
- [6] T. Shima, K. Takanashi, Y.K. Takahashi, K. Hono, Appl. Phys. Lett. 85 (2004) 2571.
- [7] M.H. Hong, K. Hono, M. Watanabe, J. Appl. Phys. 84 (1998) 4403.
- [8] K. Kang, Z.G. Zhang, T. Suzuki, C. Papusoi, J. Appl. Phys. 95 (2004) 7273.
- [9] A.C. Sun, P.C. Kuo, S.C. Chen, C.Y. Chou, H.L. Huang, Jen-Hwa Hsu, J. Appl. Phys. 95 (2004) 7624.
- [10] An-Cheng Sun, P.C. Kuo, Jen-Hwa Hsu, H.L. Huang, Jui-Ming Sun, J. Appl. Phys. 98 (2005) 076109.
- [11] J.S. Chen, Yingfan Xu, J.P. Wang, J. Appl. Phys. 93 (2003) 1661.
- [12] Yu-Nu Hsu, Sangki Jeong, David E. Laughlin, David N. Lambeth, J. Appl. Phys. 89 (2001) 7068.